Research Square

Preprints are preliminary reports that have not undergone peer review.
They should not be considered conclusive, used to inform clinical practice,
or referenced by the media as validated information.

An Interpretable AI Approach for Machine Fault DiagnosisUsing Dynamic Gradient LRP and Guided Grad-CAM withThermography

Sibi Mathew

sibimathew2019@gmail.com

TKM College of Engineering

Aneesh G Nath

TKM College of Engineering

Shyna A

TKM College of Engineering

Research Article

Keywords: Fault diagnosis, Rotating machinery, Non- Rotating machinery, Three-phase electric motors, Trans- formers, Thermal imaging, Guided Grad-CAM, Layer-wise Relevance Propagation, Explainable AI(XAI)

Posted Date: July 11th, 2024

DOI: https://doi.org/10.21203/rs.3.rs-4707414/v1

License: This work is licensed under a Creative Commons Attribution 4.0 International License.
Read Full License

Additional Declarations: No competing interests reported.

An Interpretable AI Approach for Machine Fault Diagnosis Using Dynamic Gradient LRP and Guided Grad-CAM with Thermography

Sibi Mathew
MTech Scholar,
Department of CSE
TKM College of Engineering
22082@tkmce.ac.in

Aneesh G Nath
Associate Professor,
Department of CSE
TKM College of Engineering
aneeshgnath@tkmce.ac.in

Shyna A
Assistant Professor,
Department of CSE
TKM College of Engineering
shyna@tkmce.ac.in

***Abstract*-In the realm of heavy machine operations, the necessity for efficient fault diagnosis methodologies is evident, given the substantial risks posed by breakdowns in terms of costs, manpower resources, and time. This study leverages VGG16, guided Grad-CAM, and LRP techniques for fault diagnosis in three-phase induction motors and transformers. Departing from traditional methods, this research strategically incorporates non-destructive techniques such as thermal imaging. The methodology entails training a model on a thermal image dataset using the pre-trained VGG16 architecture. Subsequently, guided image datasets are generated through the Guided Grad-CAM process, complemented by corresponding LRP data, forming the foundation for training various CNN architectures with a softmax classifier for fault categorization. Significantly, this integrated approach enables the identification of potential fault areas based on thermal gradients. Preliminary results demonstrate promising outcomes, underscoring the efficacy of this methodology in fault diagnosis. Moreover, extending beyond machinery applications, this study advocates for the integration of neural networks and thermal imaging in industries, offering prospects for predictive maintenance and enhanced operational efficiency in industrial diagnostics.**

***Index Terms*—Fault diagnosis, Rotating machinery, Non-Rotating machinery, Three-phase electric motors, Transformers, Thermal imaging, Guided Grad-CAM, Layer-wise Relevance Propagation, Explainable AI(XAI)**

I. Introduction

The rise of Industry 4.0 has brought about a whole new era of automation, data exchange, and manufacturing technologies that are completely transforming how industries operate. With the increasing reliance on complex machinery, it's absolutely crucial to have effective fault diagnosis methods in place to avoid expensive downtimes and ensure everything runs smoothly. The global industrial machinery market is seeing a huge growth spurt, thanks to the expansion of manufacturing sectors and infrastructure development all around the world[43]. This surge highlights the growing need for reliable and efficient machinery, which, despite their vital role, are still prone to faults that can cause major disruptions, financial losses, and safety risks.

In the context of Industry 4.0, traditional fault diagnosis approaches, which often involve manual inspections and invasive testing, are becoming obsolete due to their resource-intensive nature and susceptibility to human error. These methods not only disrupt operations but also fail to provide comprehensive insights into the internal conditions of machinery, limiting their effectiveness in early fault detection. This is particularly concerning given the rising adoption of motors and the aging of transformers, both of which are integral to various industrial applications.

To overcome these limitations, non-intrusive techniques such as thermal imaging have gained traction. Thermal imaging captures the heat distribution of machinery components, allowing for the early detection of temperature anomalies that may indicate potential faults. This proactive approach facilitates timely interventions before minor issues escalate into major failures.

Recent advancements in machine learning and image processing have enabled the analysis of thermal images for fault detection. However, many existing methods require manual adjustments and struggle with complex fault scenarios. In response to these challenges, this research integrates deep learning with thermal imaging to enhance fault diagnosis. Despite significant progress, challenges related to the interpretability, transparency, and efficiency of these methods remain.

This study proposes an advanced methodology for fault diagnosis in transformers and induction motors, leveraging the interpretability of Guided Grad-CAM and Layer-wise Relevance Propagation (LRP) scores. The

main contributions of this work are as follows:

- **Region of Fault Identification**: Combining Guided Grad-CAM and LRP to accurately identify fault regions in thermal images, offering actionable insights into the root causes of faults.
- **Score-Based Classification with LRP**: Implementing a score-based classification system to enhance fault prediction accuracy and provide a clear understanding of the model's decision-making process.
- **Custom LRP Model with Gradient as a Score Measure**: Utilizing gradient information to refine relevance scores, improving sensitivity to patterns indicative of machine faults.
- **Enhanced Interpretability**: Employing Guided Grad-CAM to generate visual explanations, elucidating regions of interest in thermal images associated with specific fault conditions.
- **Efficiency and Resource Optimization**: Leveraging pre-trained deep learning models and non-destructive thermal imaging to streamline the diagnostic process and reduce resource requirements.

The structure of this paper is as follows: Section 2 presents a comprehensive literature review, synthesizing existing research in the field. Section 3 outlines the proposed methodology, detailing the approach used to meet the research objectives. Section 4 describes the datasets utilized and discusses the experimental results obtained. Finally, Section 5 concludes the paper by summarizing the key findings, drawing conclusions from the results, and offering insights into potential future research directions.

II. Literature Review

In the field of fault diagnosis of industrial machinery, numerous noteworthy studies have offered valuable insights and pioneering methodologies. Al-Musawi et al. [2] presented a method for detecting faults in three-phase induction motors using thermal image segmentation and the HSV colour model. Their approach accurately identified motor faults based on temperature variations, showcasing potential applications in diverse areas.

Shao et al. [3] proposed an intelligent fault diagnosis framework for rotor-bearing systems using a modified CNN with transfer learning and infrared thermal images. The method, incorporating stochastic pooling and a Leaky Rectified Linear Unit, demonstrated superior performance in rotor-bearing fault diagnosis compared to state-of-the-art alternatives at that time.

Choudhary et al. [4] proposed an automatic, non-invasive thermal imaging approach for bearing fault diagnosis in induction motors. The methodology utilized 2D Discrete Wavelet Transform for preprocessing thermal images, Mahalanobis distance for feature selection, and Support Vector Machine for bearing condition classification. Experimental results demonstrated promising performance in accurately detecting various bearing faults, contributing to effective early fault diagnosis using thermal imaging.

Choudhary et al. [5] introduced a non-invasive thermal image-based method for bearing fault diagnosis in rotating machines. Focusing on rolling-element bearings under different conditions, including healthy and faulty scenarios, the research conducted a comparative analysis of shallow and deep learning methods. The employed Convolutional Neural Network (CNN), structured based on the LeNet-5 model, outperformed the Artificial Neural Network (ANN) in bearing fault diagnosis. The study concluded that infrared thermography provided a non-contact means for early fault detection, minimizing system shutdowns caused by bearing failures.

Glowacz et al. [6] introduced innovative fault diagnostic techniques for three-phase induction motors, emphasizing the economic impact of motor faults on production disruptions.

Hernández et al. [7] integrated thermal images and metaheuristic algorithms for failure detection in electronic systems, enhancing the accuracy of detection processes.

Janssens et al. [9] emphasized the significance of infrared imaging in condition monitoring and introduced an automatic fault detection system centered on infrared imaging, particularly focusing on bearings in rotating machinery.

Jia et al. [10] proposed an innovative fault diagnosis approach for rotating machinery using infrared thermography (IRT). Their method, based on image feature extraction with BoVW and CNN, outperformed traditional vibration-based methods in fault diagnosis accuracy, addressing challenges related to sensor installation and signal noise.

Najafi et al. [11] proposed an innovative fault diagnosis approach for electrical equipment using thermal imaging and interpretable machine learning. Their fully automated pipeline addressed challenges in varying heat dissipation patterns, categorizing data into 'cold' and 'hot' thermal states.

Khanjani and Ezoji [12] presented an automated technique for detecting operational faults in three-phase induction motors using thermal images. The non-invasive method involved SIFT-based key-point matching in thermograms, generating feature vectors with a pre-trained convolutional neural network. K-means clustering and an SVM-based classifier achieved a 100

H.-Y. Chen and C.-H. Lee [13] introduced an innovative approach that combined Explainable Artificial Intelligence (XAI) with Convolutional Neural Networks (CNNs) for bearing faults diagnosis. The methodology transformed vibration signals into images using Short-Time Fourier Transform (STFT), employing a CNN as the classification model. Gradient Class Activation Mapping (Grad-CAM) generated attention maps, providing insights into the model's decision-making process.

Selvaraju et al. [14] proposed Guided Grad-CAM, enhancing the interpretability of deep learning models by visualizing and highlighting regions within images contributing to a model's decision.

Johnson et al. [21] employed transfer learning techniques, adapting pre-trained models to fault diagnosis tasks. Their approach demonstrated the feasibility of leveraging existing knowledge to enhance diagnostic model performance.

Despite the advancements in fault diagnosis methodologies, existing approaches faced challenges related to interpretability, transparency, and efficiency. Many methods lacked the ability to provide clear insights into the decision-making process of the models, hindering their practical applicability.

To address these challenges, this work introduced an innovative methodology that not only enhanced interpretability but also contributed to the efficiency of the fault diagnosis process through the identification of possible fault regions.

III. Proposed System

The proposed system integrates thermal imaging with advanced deep-learning techniques to enhance the detection of faults in three-phase induction motors. The architecture, illustrated in Figure 1, involves a strategic combination of Guided Grad-CAM and Layer-wise Relevance Propagation (LRP) methodologies, fostering a comprehensive and interpretable approach to fault diagnosis.

A. Architecture

The architecture proposed for fault diagnosis in three-phase induction motors and transformers integrates advanced techniques in deep learning, visualization, and classification to provide a comprehensive solution for early fault detection. Beginning with data acquisition and preprocessing, thermal images are prepared through resizing, normalization, and augmentation to ensure dataset uniformity and diversity. Leveraging the feature extraction capabilities of the pre-trained VGG-16 network, high-level features crucial for fault diagnosis are captured from the thermal images. Visualization techniques such as Grad-CAM and Guided Grad-CAM generate heatmaps highlighting regions of interest, while Layer-wise Relevance Propagation (LRP) derives pixel-wise relevance scores, enriching the dataset with both visual insights and detailed pixel-level information. This combined dataset is then fed into a meticulously designed Convolutional Neural Network (CNN), which refines its parameters through training to recognize and prioritize relevant patterns within the thermal images. Finally, a Softmax classifier interprets the features extracted by the CNN to predict the fault type or health status of the machinery, along with indicating the region of fault.

B. Preprocessing

The preprocessing phase is a critical step in preparing the thermal image dataset for subsequent fault detection in machinery. It involves several key processes aimed at optimizing the dataset's quality and diversity to enhance the model's performance. The initial step is resizing the images to a consistent dimension, such as (224, 224) pixels, to ensure uniformity and alignment with the model's input requirements. Shuffling the dataset helps prevent any inadvertent bias during training and evaluation, enabling the model to learn from a varied set of samples. To improve model generalisation and robustness, data augmentation[48] techniques are also applied. Additionally, normalisation is crucial for standardising pixel values across images, usually within a range of 0 to 1 or -1 to 1. This step ensures stable and efficient model training by preventing input values from dominating the learning process. Also if certain areas of the images are irrelevant to the fault detection task, manual or automated extraction of the region of interest (ROI) can improve the signal-to-noise ratio and enhance model performance. Furthermore, addressing noise present in thermal images is essential. Techniques like Gaussian or median filtering can be employed to reduce noise while preserving essential features.

C. Pre-Trained CNN as a Feature Extractor

This proposed system, seamlessly integrates the pre-trained VGG16 model with the Guided Grad-CAM technique, enhancing the interpretability and transparency of the fault detection process for three-phase induction motors. The work begins with the fine-tuned VGG16 model, adapting its general image understanding capabilities to the specific task of fault detection. During training, the initial layers—responsible for low-level feature

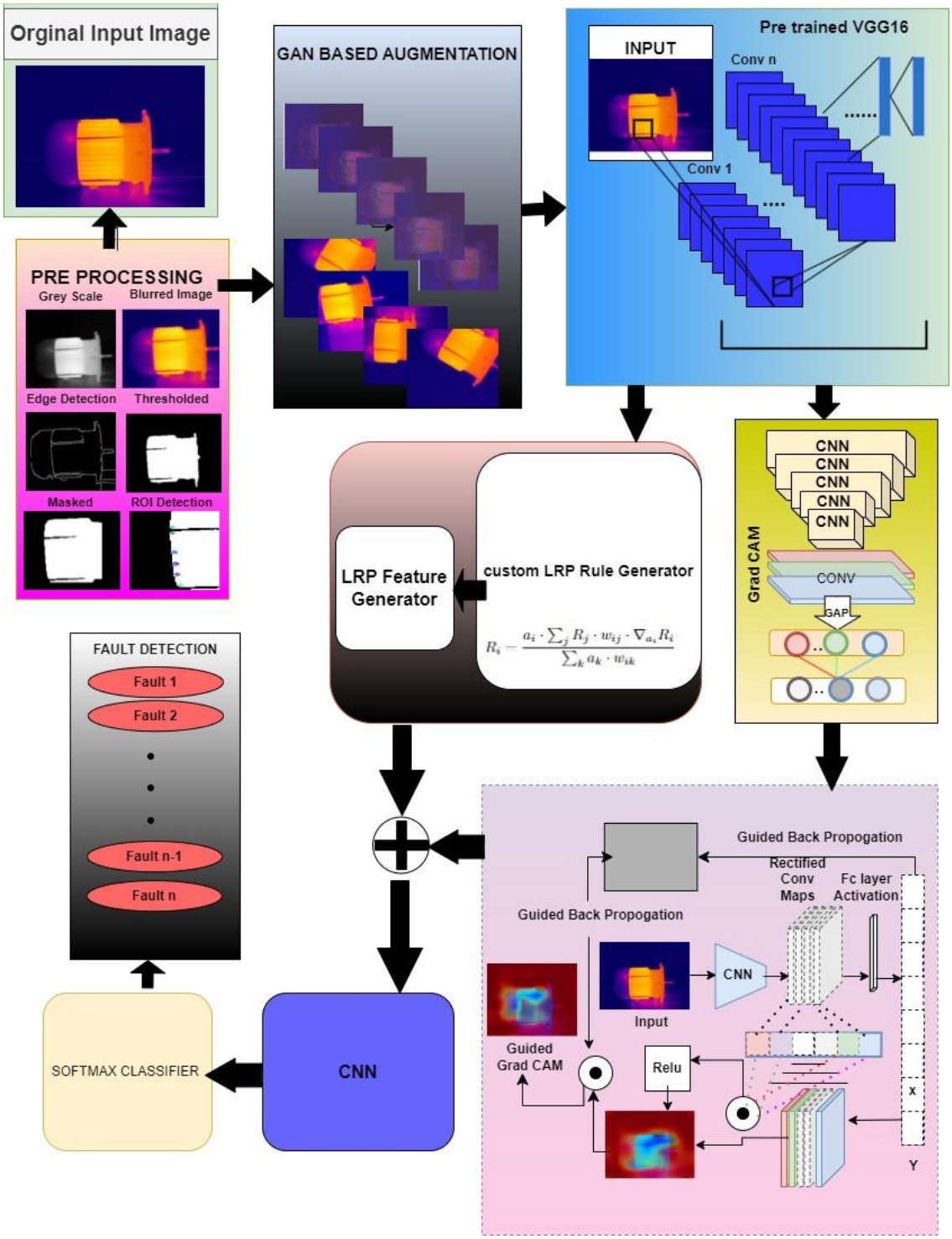

Fig. 1: Architectural Diagram of the proposed system

detection—remain unaltered. However, the final fully connected layers, designed for ImageNet classification, are replaced by a customised classifier tailored to the 11 fault classes in the thermal image dataset. This transfer-learning approach enables the model to capture thermal patterns indicative of different motor faults.

Once prepared, the VGG16 model serves as a feature extractor. Each thermal image undergoes meticulous analysis as the model traverses its layers, capturing high-level features encapsulating pertinent thermal patterns and structures.

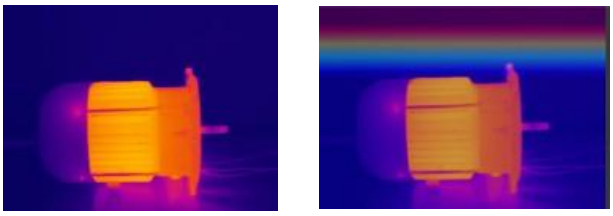

(a) Original Image (b) CAM image

Fig. 2: CAM generated image

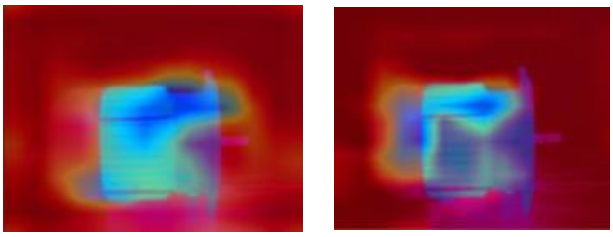

(a) Grad-Cam Image (b) Guided Grad-CAM image

Fig. 3: Grad Cam image for Guided Grad CAM

D. Utilization of Guided Grad CAM

The Guided Grad-CAM images, enriched with visual cues highlighting crucial fault-related regions within thermal images, play a pivotal role in enhancing the classification accuracy and interpretability of this system.This block generates Guided Grad-CAM images for each thermal image using the pre-trained VGG16 model. These images encapsulate localised visual cues, effectively capturing intricate patterns indicative of different motor faults. These images are seamlessly integrated into a CNN model tailored for classification tasks. Guided Grad-CAM, a synergy of Grad-CAM and Guided Backpropagation, takes center stage in generating heatmaps illuminating regions within thermal images significant for the model's classification decision. Grad-CAM identifies relevant regions using gradient information, while Guided Backpropagation refines the visualisation, focusing exclusively on positive contributions.

E. Utilization of Layer-wise Relevance Propagation (LRP)

The utilization of Layer-wise Relevance Propagation (LRP) in conjunction with Guided Grad-CAM enhances the interpretability and accuracy of the proposed fault detection system[40].

1) Distinctive LRP Implementation

The LRP approach employed here distinguishes itself through the integration of custom LRP gradient scores, meticulously crafted for fault detection using thermal images . While LRP serves as a potent tool for assigning relevance scores to neurons, this method surpasses conventional practices by addressing the nuanced challenges within the industrial machinery domain. This work customizes LRP scores to capture subtle features indicative of faults, incorporating specialized handling of gradient information. This ensures that the relevance scores precisely reflect critical regions in thermal images related to specific fault conditions. By fine-tuning LRP gradient scores to the intricacies of industrial machinery, elevate the precision and effectiveness of fault diagnosis, making this approach uniquely suited for the challenges posed by machines.

2) Consideration of Gradient Dynamics in LRP

Within this custom LRP implementation, the consideration of gradients plays a pivotal role in determining relevance scores. In the context of LRP, the relevance score (R_i) for a neuron in a specific layer is determined by the interplay of activations (a_i), weights (w_{ij}), and relevance scores from the next layer (R_j). The relevance propagation formula is expressed as:

$$R_i = \frac{a_i \cdot \sum_j R_j \cdot w_{ij}}{\sum_k a_k \cdot w_{ik}}$$

The gradient ($\nabla_{a_i} R_i$), representing the sensitivity of the relevance score to changes in the neuron's activation, becomes a crucial factor. In this customization, this work carefully consider gradient information to enhance the discriminatory power of relevance scores in the context of fault detection.

The adapted relevance propagation with gradient can be expressed as:

$$R_i = \frac{a_i \cdot \sum_j R_j \cdot w_{ij} \cdot \nabla_{a_i} R_i}{\sum_k a_k \cdot w_{ik}}$$

The inclusion of the gradient term in the numerator refines the relevance score by considering the sensitivity of the score to changes in the neuron's activation. This

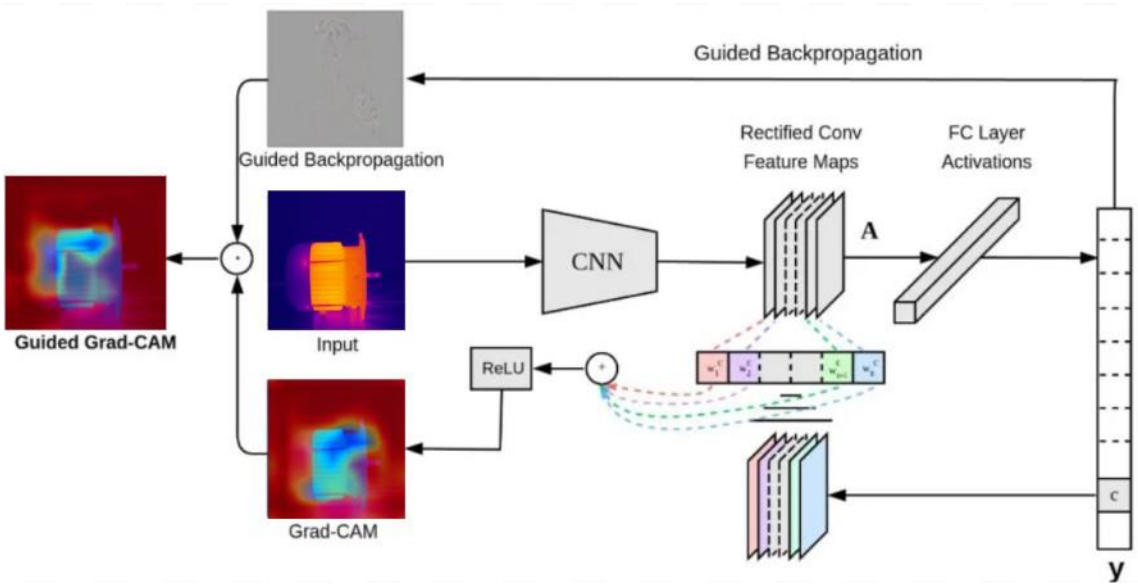

Fig. 4: Guided Grad Cam[32]

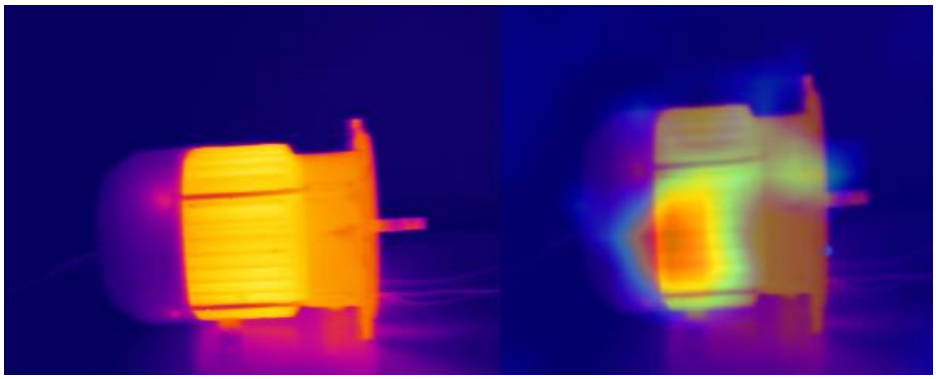

(a) Original Image (b) Guided Grad CAM image

Fig. 5: Shows transition from the original image to the guided image

customization ensures that the relevance scores not only consider the importance of connections (weights) and the contribution of neurons in the next layer (R_j), but also factor in the gradient information, making them more attuned to the specific patterns indicative of faults.

F. Integrated LRP-Guided Grad-CAM

The LRP scores obtained for each layer seamlessly combine with Guided Grad-CAM images during the fault classification process. Guided Grad-CAM generates heatmaps that highlight regions of faults in thermal images. The fusion of LRP scores with Guided Grad-CAM images creates a comprehensive dataset that combines pixel-wise and layer-wise relevance. This strategic integration enhances the interpretability and accuracy of fault detection system in identifying the region of fault.

G. Classification Using CNN and Softmax Classifier

Convolutional Neural Networks (CNNs)Fig4 along with a Softmax classifier forms the core of the proposed fault classification system. The CNN architecture is tailored to process combined datasets, capturing intricate localized features indicative of faults. This architecture comprises convolutional layers to detect spatial patterns, pooling layers for downsampling, fully connected layers for high-level abstraction, and a Softmax classifier for generating class probabilities.This is particularly useful for tasks like multi-class classification, where the

softmax output can be interpreted as class probabilities, aiding in the prediction During training, the CNN learns to associate unique patterns with fault classes, refining its weights through optimization techniques. The trained CNN predicts fault classes for new images, with accuracy assessed using metrics like accuracy score.This integrated approach maximizes the interpretability of images, facilitating precise and reliable fault classification.

Algorithm: Fault Detection

Input:

- I = $\{I_1, I_2, \ldots, I_n\}$: Set of thermal images
- Image size = (224, 224)
- class_labels = $\{c_1, c_2, \ldots, c_{11}\}$
- data = np.array

Procedure:

1) Shuffle the dataset: $data, labels = shuffle(data, labels)$
2) Preprocess input images for VGG16: $data = preprocess\_input(data)$
3) Load VGG16 model: $vgg16\_model = VGG16(weights = 'imagenet', include\_top = False, input\_shape = (224, 224, 3))$
4) For each image:
   - Apply the Guided Grad-CAM technique to generate heatmaps for each thermal image: $R_{GuidedGradCAM} = \{GuidedGradCAM(I_1), GuidedGradCAM(I_2), \ldots, GuidedGradCAM(I_n)\}$
   - Use the pre-trained VGG16 model to produce Grad-CAM images: $R_{GradCAM} = \{GradCAM(I_1), GradCAM(I_2), \ldots, GradCAM(I_n)\}$
   - Refine Grad-CAM images using Guided Backpropagation: $R_{GuidedBackprop} = \{GuidedBackprop(GradCAM(I_1)), GuidedBackprop(GradCAM(I_2)), \ldots, GuidedBackprop(GradCAM(I_n))\}$
   - Customize LRP scores for fault detection: $LRP\_scores = CustomLRP(features)$ for each image
5) For each LRP data and Guided Grad-CAM, combine both:
   - Design a CNN architecture to process combined Guided Grad-CAM-LRP images: $CNN\_model = DesignCNN(R_{GuidedGradCAM\text{-}LRP})$

Output Visualization:

- Visualize classification results with Guided Grad-CAM images and LRP relevance scores: $Visualization(C_{predicted}, R_{GuidedGradCAM\text{-}LRP})$
- Provide domain experts with visually highlighted regions of interest for validation.

Output:

- Classification results and highlighted regions of interest for validation.

IV. Experimental Results and Discussion

This section provides an overview of the key elements driving the success of fault detection research. This work is initiated by presenting a detailed description of the dataset used as the foundation of this study, shedding light on its origins, characteristics, and preprocessing techniques. Subsequently, this study delves into the intricacies of the experimental setup, elucidating the methodologies, algorithms, and parameter configurations employed to develop and assess fault detection systems. Finally, it presents both quantitative and qualitative results, offering a clear and insightful evaluation of the effectiveness and practicality of the proposed solution.

A. Dataset

The dataset used in this study originates from the Babol Noshirvani University of Technology. It is tailored for fault diagnosis through thermal imaging and is designed to support academic and research pursuits. The dataset focuses on condition monitoring for electrical equipment, specifically Induction Motors[23] and Transformers[41]. Thermal images were acquired using the Dali-tech T4/T8 infrared thermal image camera under controlled conditions[11] as depicted in the Table I.

Dali-tech T8 TIC	
Detector resolution	384*288
Measurement accuracy	±2°C or ±2% (of reading)
Imaging NETD	≤ 0.04°C@30°C
Measuring range	-20°C - 650°C
Imaging Frame Rate	50/60Hz

TABLE I: Specifications of the Dali-tech T8 TIC thermal imaging camera

1) Induction Motor Dataset

The dataset experiments were conducted on a three-phase induction motor whose specifications can be noted from the table II where the motor was short-circuited

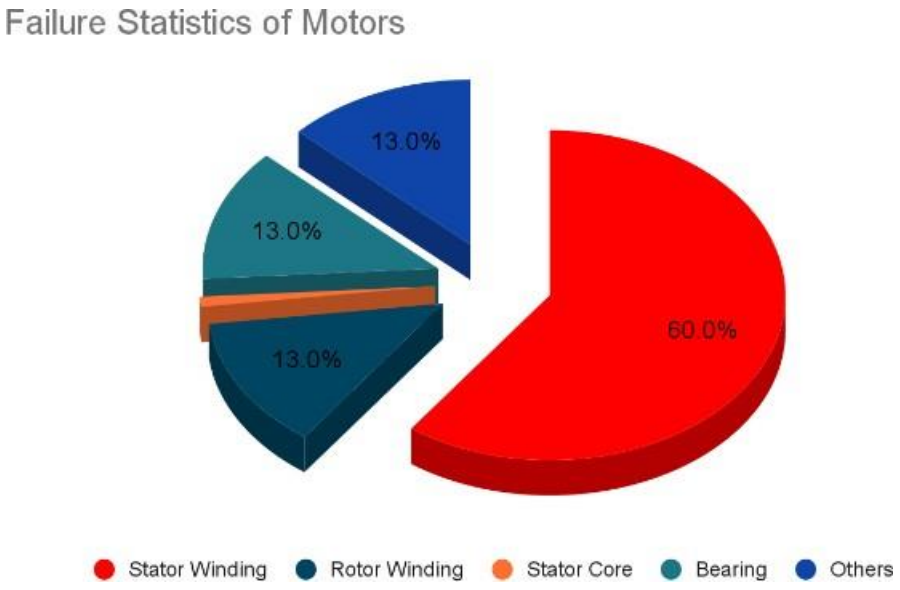

Fig. 6: Chances of occurrence of fault from survey in motor

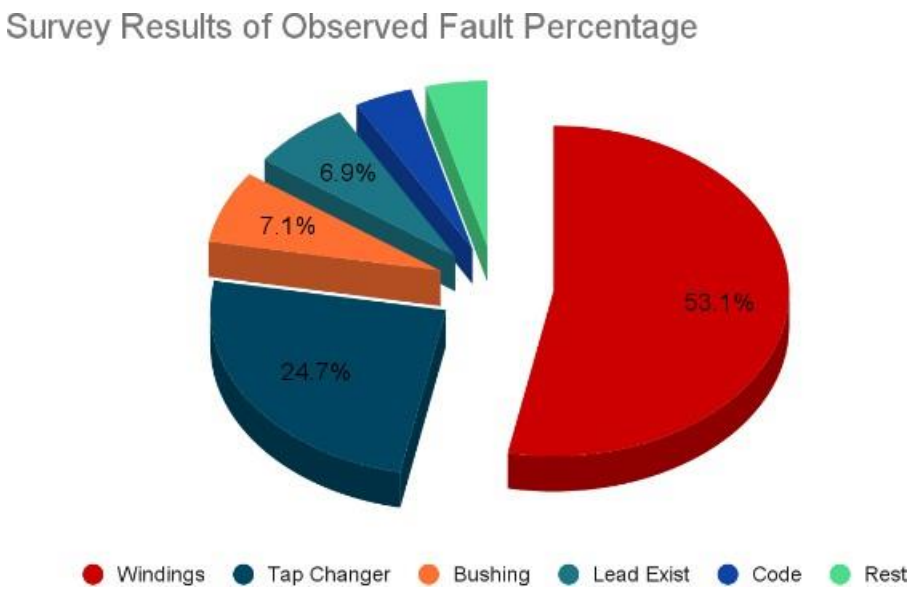

Fig. 7: Chances of occurrence of fault from survey in transfomer

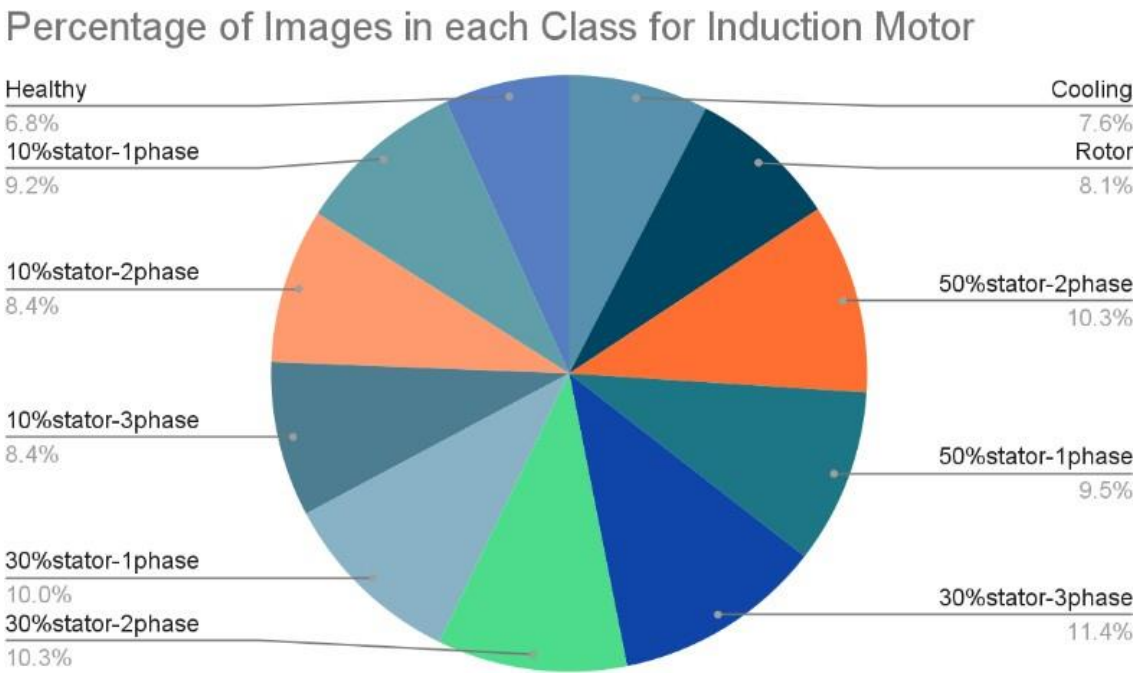

Fig. 8: Fault distribution across classes in Induction Motor Dataset

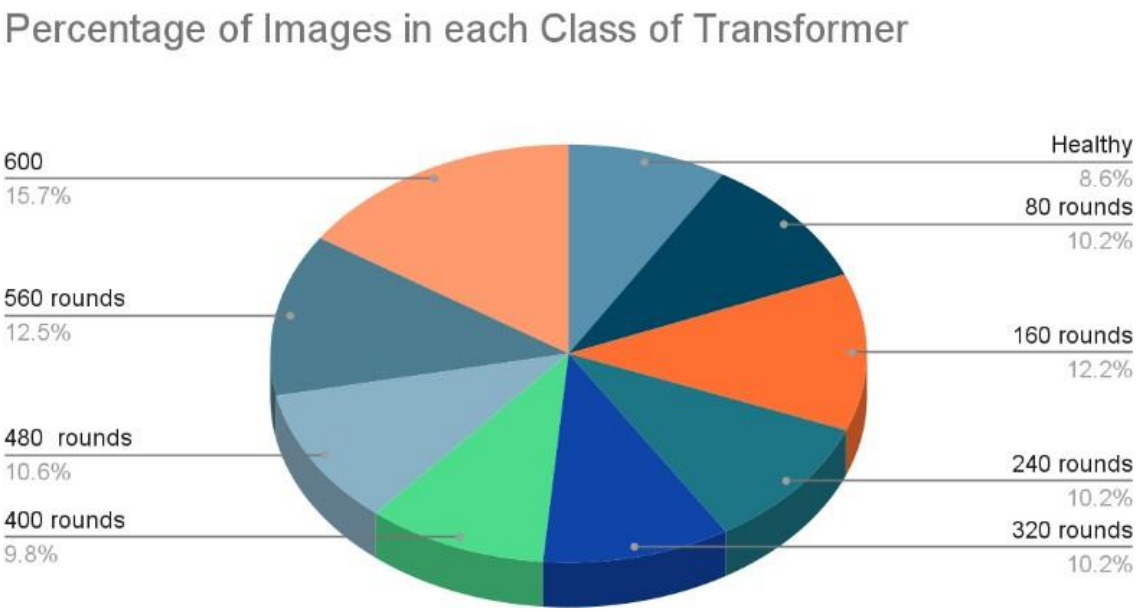

Fig. 9: Fault distribution across classes in Transformer Dataset

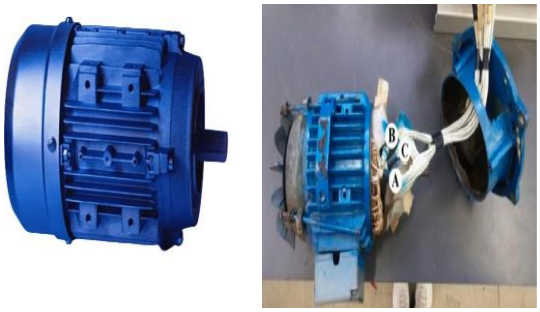

(a) (b)

Fig. 10: Internal structure of Experimented Motor

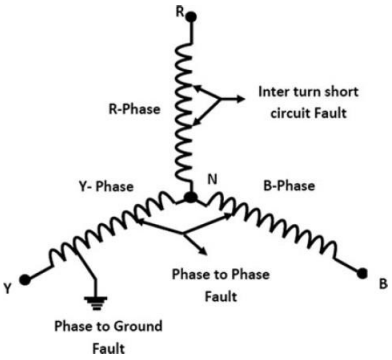

Fig. 11: Ciruit Datail for motor short Dataset

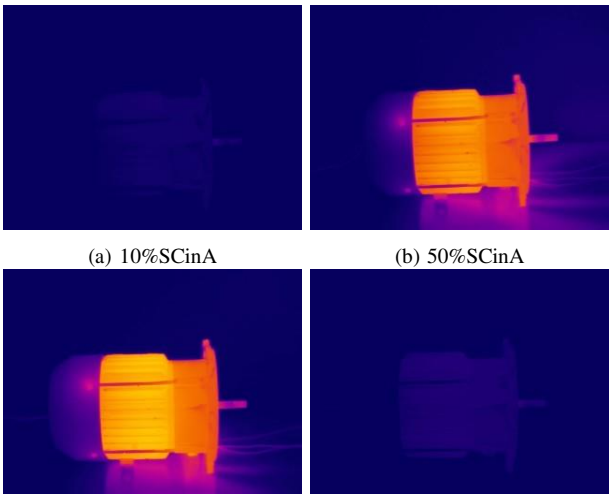

(a) 10%SCinA (b) 50%SCinA

(c) 30%SCinA&B&C (d) 10%SCinA&B

Fig. 12: Sample Dataset Induction Motor[29]

Fig. 13: Similar transformer used for experiment

at different winding sections, as depicted in Figure 10. Sections marked A, B, and C represent the short-circuited stator winding phases used for experimental purposes. The details of the experimental circuit can be seen in Figure **??**, as referenced in study [51].

The dataset was created to specifically address faults in the winding, as studies have shown that windings are a common cause of motor faults [49], which is clearly illustrated in Figure **??**. The thermal images in this dataset are distributed across 11 unique fault classes of induction motors, as shown in Figure 8. These scenarios represent the motor in both ”no-load” and ”coupled-with-generator” states. The various fault classes include short circuits in different phases, cooling fan faults, and rotor faults.

2) Transformer Dataset

The dataset for transformers was produced using a similar transformer as shown in Figure 13, which is a dry-phase shell-type transformer. The dataset was collected based on faults in the winding, with different classes created for various sets of short-circuited conditions under both load and no-load conditions. It is important to study winding faults, as windings are prone to faults according to studies [50], as illustrated in Figure 7. The transformer can be short-circuited under load conditions, as shown in Figure 14, as observed from study [52]. The experimental dataset was built under nine distinct conditions, one of which is the healthy state. The distribution of images can be observed from Figure 9. This dataset focuses on internal faults, particularly short circuit failures in the common core winding, as noted in study [11]. The specifications of the transformer are detailed in Table II, and the images were captured on a laboratory workbench.

Transformer		Induction Motor	
Phase	1	Phase	Y 3
Power	1KW	Power	1.1KW
Voltage	220V	Voltage	220/380V
Input Current	1.5A	Input Current	5A
Operating Voltage	220-660	Speed	2800RPM
Frequency	50-60Hz	Frequency	50Hz

TABLE II: Specifications of Transformer and Induction Motor[11]

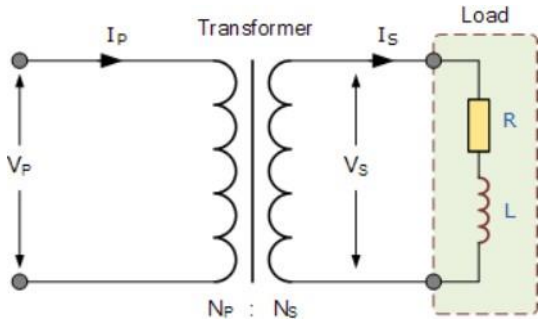

Fig. 14: Circuit of transformer under oad condition

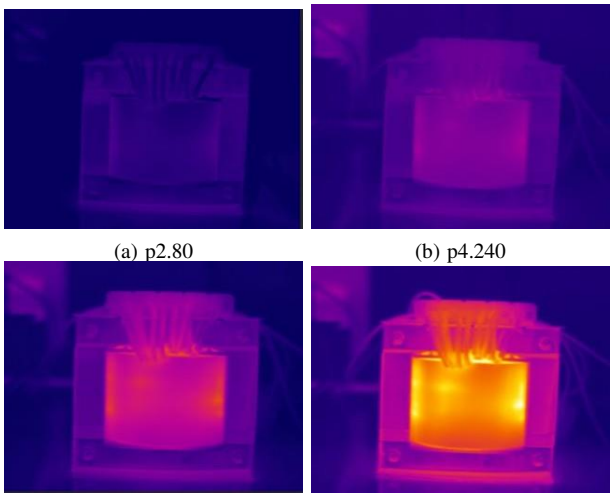

(a) p2.80 (b) p4.240

(c) p6.400 (d) p9.600

Fig. 15: Sample Dataset Transformer[41]

B. Data Preparation and Model Training

This experiment explores the utilization of Neural Networks for image classification and fault diagnosis. The images were resized to a uniform size of 224x224 pixels to match the input size required by the VGG16 model. To establish a baseline for comparison, the dataset was split into training and testing sets using an 80%-20% ratio, ensuring a diverse representation of classes in both sets. A random seed value of 42 was used to ensure the reproducibility of results.

The CNN architecture comprises two convolutional layers, with the first layer having 32 filters and the second layer having 64 filters. Each convolutional layer was followed by a max-pooling layer with a pool size of (2, 2). A fully connected layer with 128 units and a ReLU activation function was employed before the final output layer, which used the softmax activation function to predict class probabilities. During training, the VGG16 model was compiled using the Adam optimizer and sparse categorical cross-entropy loss function. The training was conducted with a batch size of 32 samples. To monitor model performance and prevent overfitting, a validation split of 10% was used during training.

Guided Grad-CAM was employed to visualize the regions of interest in the images that contribute to the model's predictions. The Grad-CAM heatmap was generated from the 'block5_conv3' layer of the VGG16 model, and guided backpropagation was used to compute gradients for highlighting these regions. Additionally, the Guided Grad-CAM dataset was generated by applying the Guided Grad-CAM technique to each image in the original dataset. Similarly, an LRP dataset for each image was also produced using appropriate functions. These two datasets were then combined to produce a new dataset. This new dataset was split into training and testing sets using the same 80%-20% ratio, and the images were preprocessed by scaling their pixel values to the range [0, 1].The CNN model was then trained on the combined dataset. The model's performance was evaluated on the test set using the softmax classifier. The predicted class probabilities were obtained and compared with the ground truth labels to calculate the test accuracy.

C. Results

The main focus of this study revolves around the identification of faults in machines, particularly within the context of three-phase induction motors and transformers. This research endeavour has led to the development of a novel architecture designed to process thermal images as input. Through the application of Guided Grad-CAM and LRP, this architecture effectively predicts the fault class associated with the input image

and concurrently pinpoints the specific region of abnormality. By harnessing the power of guided thermal imaging and sophisticated deep learning techniques, this work establishes a comprehensive solution for robust fault identification in machines, thereby contributing to enhanced operational efficiency and maintenance practices. The result obtained analyzed as follows:

1) Quantitative Evaluation

In addition to qualitative analysis, the results can be quantitatively analyzed.

Classes	Precision	Recall	F1-score
class1(A&B50)	1.00	1.00	1.00
class2(A&B&C10)	1.00	0.88	0.93
class3(A&B&C30)	1.00	0.92	0.96
class4(A&C10)	0.83	0.83	0.83
class5(A&C300)	1.00	1.00	1.00
class6(A10)	0.80	0.80	0.80
class7(A30)	0.90	0.82	0.86
class8(A50)	0.50	0.50	0.50
class9(Fan)	1.00	1.00	1.00
class10(Noload)	0.60	1.00	0.75
class11(Rotor-0)	0.86	1.00	0.92
Accuracy			0.95

TABLE III: Result of different quantitative approaches in Induction Motors(no of epochs :20, Batch size=32)

Classes	Precision	Recall	F1-score
class1(p1 Noload)	1.00	.86	.92
class2(p2 80)	.83	1.00	0.91
class3(p3 160)	1.00	1.00	1.00
class4(p4 240)	1.00	1.00	1.00
class5(p5 320)	1.00	1.00	1.00
class6(p6 400)	1.00	1.00	1.00
class7(p7 480)	1.00	1.00	1.00
class8(p8 560)	1.00	1.00	1.00
class9(p9 600)	1.00	1.00	1.00
Accuracy			0.98

TABLE IV: Result of different quantitative approaches in Transformer(no of epochs :20, Batch size=32)

In the evaluation process, three different measurement-based metrics were utilized, and the class-wise accuracy was also studied, as shown in Figure **??**. These metrics are essential for assessing the performance of the model. The experimental results demonstrate the effectiveness of the fault diagnosis approach using guided thermal images. The classification model achieved remarkable accuracies of more than 95% on the induction motor dataset and 98% on the transformer dataset. However, there are some issues with variations in specific measures, as seen in Table III and Table IV, which are also reflected in the confusion matrices shown in Figures 19 and 20.

Upon closer observation and examination, it was noted that the images of the classes that showed variations have visual similarities, which caused slight fluctuations in the prediction performance. This indicates that while the model performs exceptionally well overall, there are challenges in distinguishing between visually similar fault classes, which can lead to minor inconsistencies in the classification results.

Additionally, Figure 18 illustrates how the model made predictions as a classification model. All the previously discussed results highlight the success of this approach. The upcoming section provides a detailed analysis in terms of qualitative results.

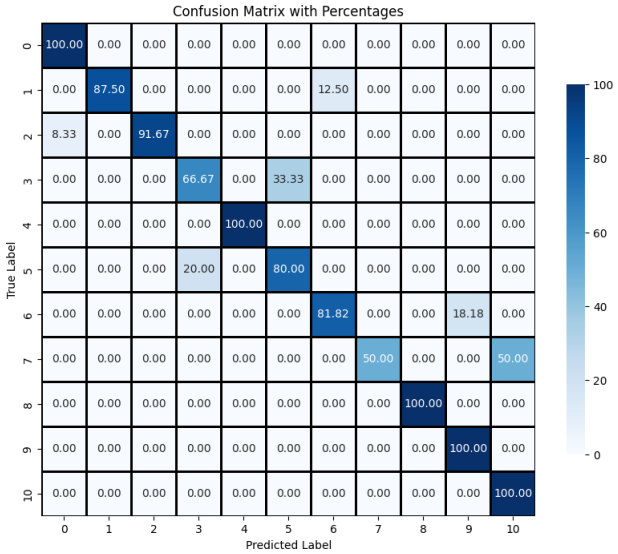

Fig. 19: Confusion matrix Induction motors

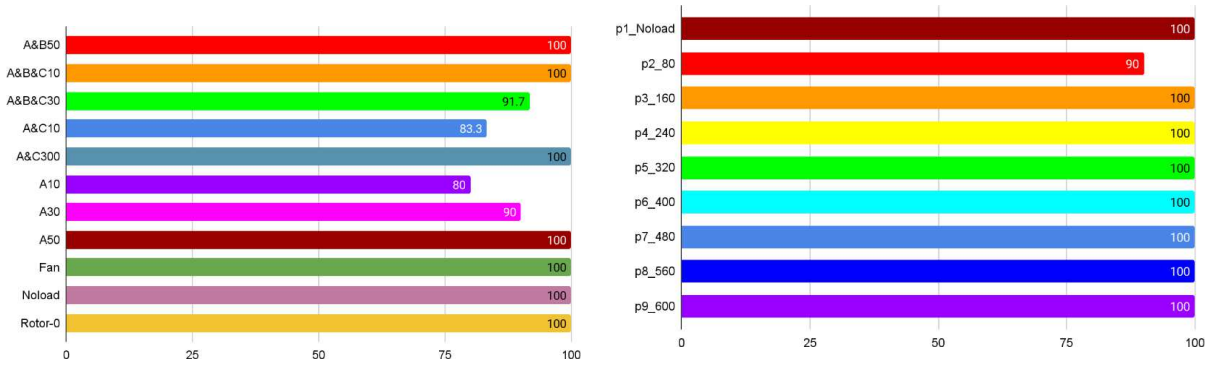

(a) Class-wise accuracy of Induction Motor

(b) Class-wise accuracy of Transformer

Fig. 16: Accuracy Comparison of Dataset

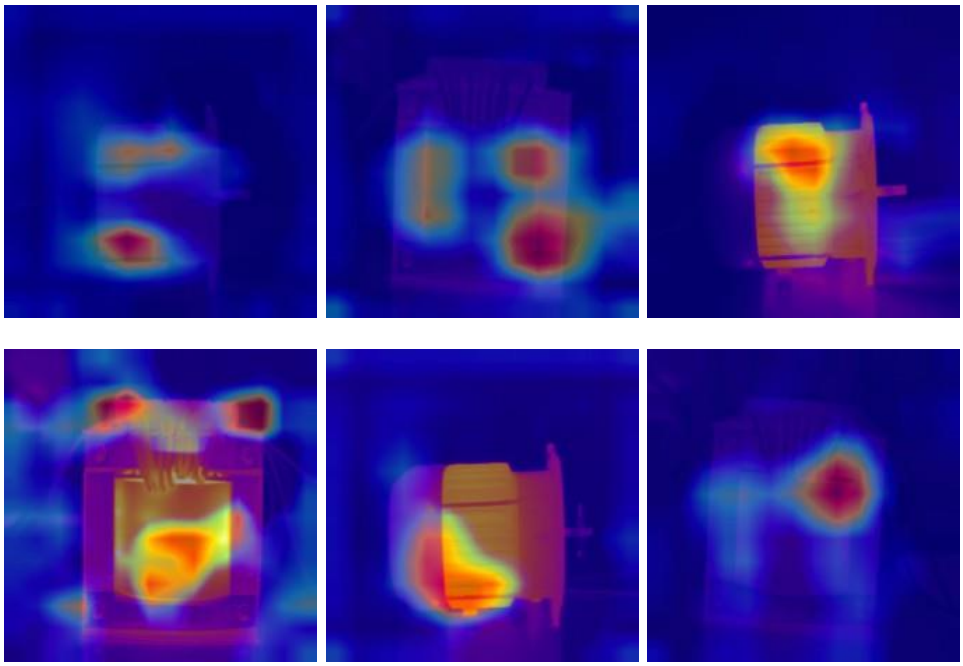

Fig. 17: Guided Grad CAM Output

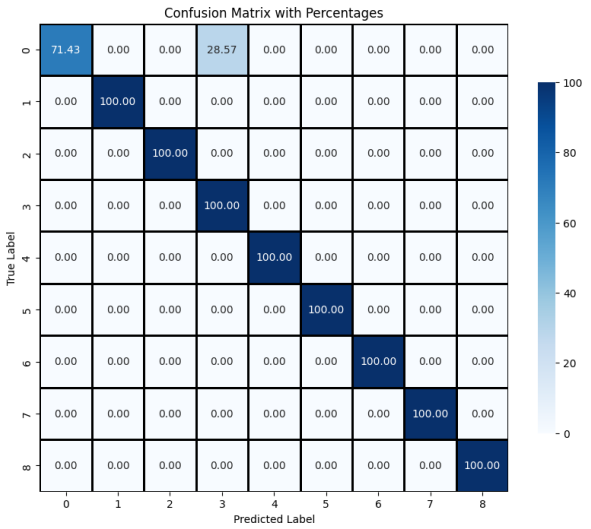

Fig. 20: Confusion matrix Transformers

2) Qualitative Analysis of Region Identification

The quantitative analysis results provide comprehensive insights into the model's prediction performance using various evaluation metrics, clearly demonstrating the model's effectiveness. The classification model achieved high accuracy rates on both the induction motor and transformer datasets, indicating its strong capability to correctly identify and classify faults.

In addition to the quantitative analysis, a qualitative analysis through visual examination further substantiates the model's capabilities. By utilizing heatmaps generated

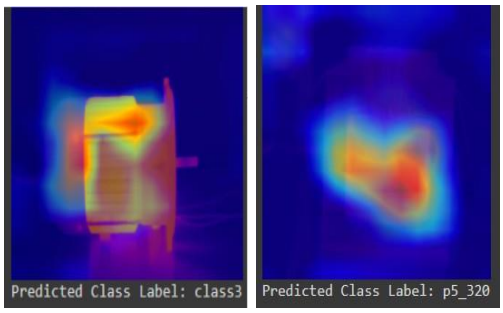

(a) (b)

Fig. 18: Prediction of Fault using Guided Grad CAM

through the Guided Grad-CAM technique, the work visually interprets the regions of interest that the model focuses on while making predictions. This interpretability is crucial for validating the model's decisions and understanding its internal workings. Figure 17 showcases these heatmaps, highlighting the specific areas that contributed to the model's fault classification decisions.This transparency is essential for gaining trust in AI models, especially in critical applications like fault diagnosis.

Furthermore, this study also assessed the capability of Guided Grad-CAM by comparing it with its predecessor, as illustrated in Figures 2 and 3. These comparisons underscore the improvements and efficacy of the Guided Grad-CAM approach, demonstrating its superior performance in highlighting relevant fault regions of interest compared to earlier methods.

The ultimate aim of this study was to identify potential fault regions accurately. To a significant extent, the model has proven its capability in achieving this goal, as depicted in Figure 21. These illustrations provide a clear visualization of the subsequent stages, starting from the input thermal images used to generate the Guided Grad-CAM, followed by the application of Dynamic Layer-wise Relevance Propagation (LRP). The combination of Guided Grad-CAM and Dynamic LRP produces intermediate heatmaps that effectively gives into the possible area of fault. This multi-stage approach ensures a more precise identification of faults by leveraging the strengths of both methods.

In the upcoming section, this work quantitatively examines the identified fault regions to ensure that these regions correspond to potential fault areas in terms of temperature gradients

3) Quantitativly Comparing Fault highlighted image

For the analysis, the original and fault-highlighted images were compared using several metrics, including gradient magnitude in terms of colour gradient and temperature intensity values. The objective was to determine whether the highlighted regions corresponded to fault areas characterized by higher temperature regions.

The mean gradient magnitude values increased from 27.74 in the original image to 50.24 in the highlighted image for the motor dataset, and from 27.62 to 97.3 for the transformer dataset. Similarly, the median gradient magnitude values increased from 42.0 to 57.0 for the motor and from 39.0 to 147.0 for the transformer Figure 22. These changes indicate a significant enhancement in gradient magnitude, suggesting that the highlighted regions effectively correspond to areas of interest.

The maximum gradient magnitude also shows an increase. Despite this, the p-value, which indicates the statistical significance of these changes, was remarkably small (1.10×10^{-184} for the motor and almost 0 for the transformer). This affirms the effectiveness of the highlighting technique in distinguishing fault regions.

In terms of temperature/intensity distribution, the mean temperature/intensity rose significantly, accompanied by a decrease in standard deviation for both datasets. This shift towards higher temperatures/intensities further reinforces the identification of fault regions. Percentile values (25th and 75th) also showed notable shifts towards higher temperatures/intensities, strengthening the conclusion that the highlighted regions are effectively indicating faults.It is important to note that some values were normalized by dividing them by 10 or 100 to facilitate effective visualization. Multiple metrics were used for comparison, as shown in Figure 22, each demonstrating higher values for the highlighted images compared to the original images.

4) Quantitatively and Qualitatively Comparing Fault Highlighted Images with original images

For the analysis, the original and fault-highlighted images were compared using several metrics, including gradient magnitude in terms of color gradient and temperature intensity values. The objective was to determine whether the highlighted regions corresponded to fault areas characterized by higher temperature regions.

The mean gradient magnitude values increased from 27.74 in the original image to 50.24 in the highlighted image for the motor dataset, and from 27.62 to 97.3 for the transformer dataset. Similarly, the median gradient magnitude values increased from 42.0 to 57.0 for the motor and from 39.0 to 147.0 for the transformer. These changes indicate a significant enhancement in gradient magnitude, suggesting that the highlighted regions effectively correspond to areas of interest.

The maximum gradient magnitude, however, showed a slight decrease from 54.49 to 75.23. Despite this decrease, the p-value, which indicates the statistical significance of these changes, was remarkably small

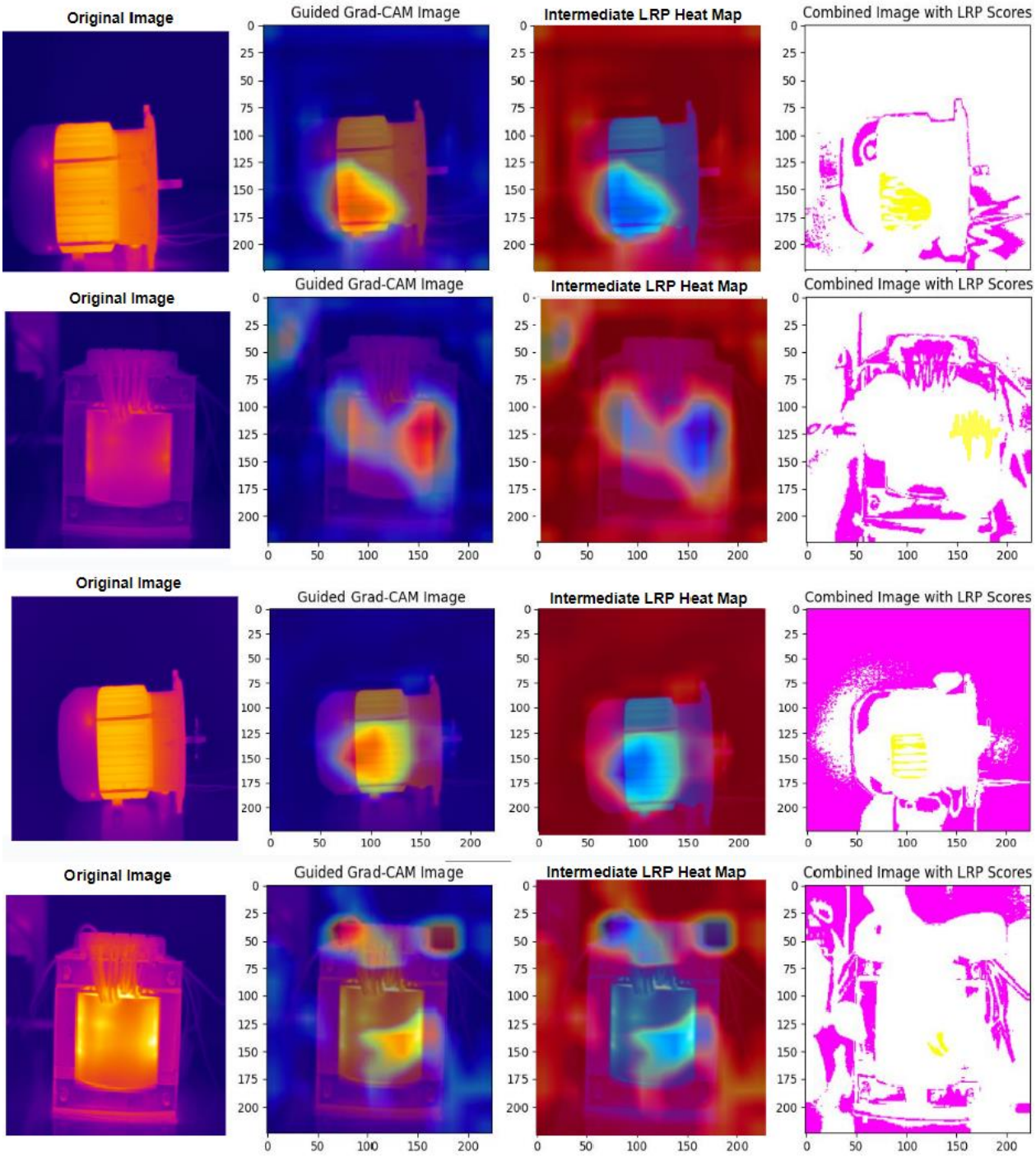

Fig. 21: Subsequent Stages Potential Fault Region Detection

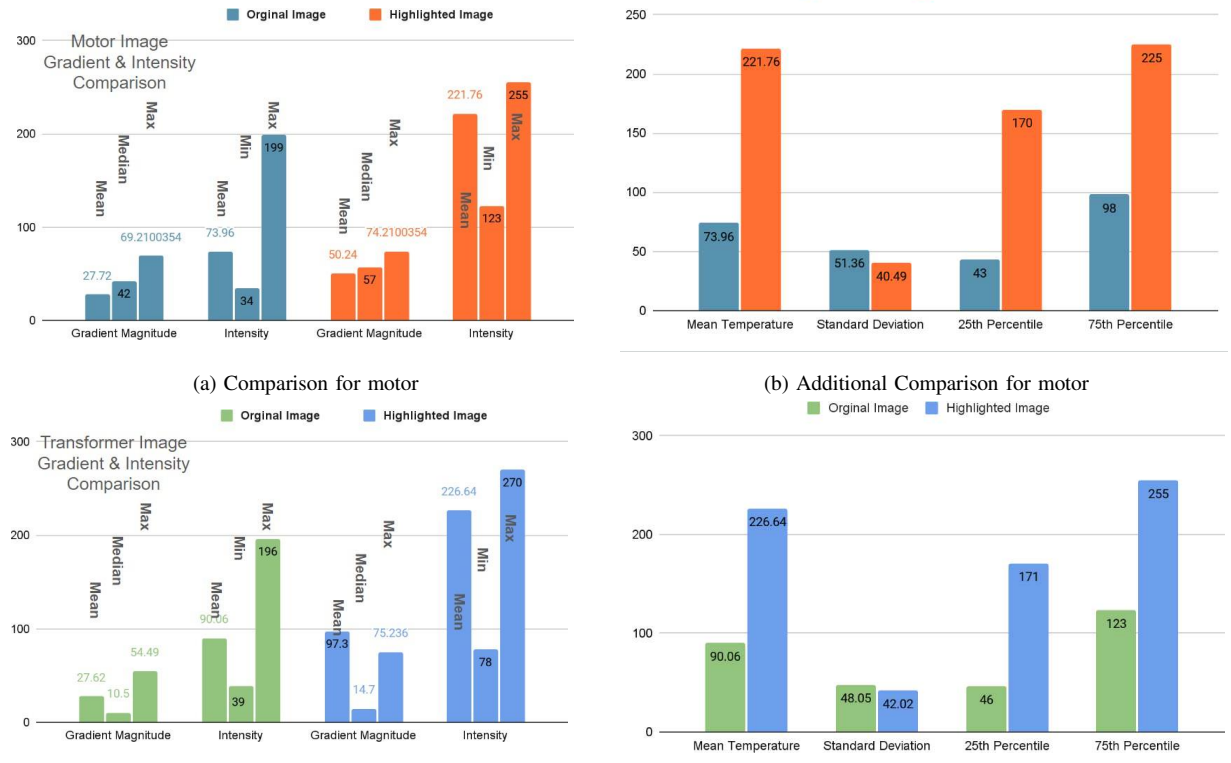

(a) Comparison for motor

(b) Additional Comparison for motor

(c) Comparison for Transformer

(d) Additional Comparison for Transformer

Fig. 22: Comparing original and highlighted image

(1.10×10^{-184} for the motor and almost 0 for the transformer). This affirms the effectiveness of the highlighting technique in distinguishing fault regions.

In terms of temperature/intensity distribution, the mean temperature/intensity rose significantly from 73.96 to 255.0, accompanied by a decrease in standard deviation for both datasets. This shift towards higher temperatures/intensities further reinforces the identification of fault regions. Percentile values (25th and 75th) also showed notable shifts towards higher temperatures/intensities, strengthening the conclusion that the highlighted regions are effectively indicating faults.

It is important to note that some values were normalized by dividing them by 10 or 100 to facilitate effective visualization. Multiple metrics were used for comparison, as shown in Figure 22, each demonstrating higher values for the highlighted images compared to the original images.

Additionally, on visual comparison, Figure 23a and Figure 23c superimpose the original and highlighted images to provide insight into the regions of fault. This superimposition allows for a direct comparison where the images coincide exactly, highlighting the areas of interest. Furthermore, Figure 23b and Figure 23d first crop out the high-intensity regions, then generate an image of gradient magnitude, which is compared with the fault-detected regions. This comparison shows that the identified fault regions fall within the high-intensity areas, providing further validation of the fault detection method.

These findings collectively demonstrate the effectiveness of the combined approach in identifying potential fault regions. This is crucial for fault detection and diagnosis in thermal images, ensuring proactive maintenance and operational reliability in industrial applications.

5) Comparing with State of Art

This study presents a unique methodology by combining Explainable AI techniques with dynamic Layer-wise Relevance Propagation (LRP), offering a novel approach to fault identification that previous methods could not achieve. Unlike earlier studies that primarily focused on the classification capabilities of convolutional networks, this research emphasizes enhancing the prediction capability by pinpointing the exact regions of faults.

The initial experiments involved evaluating several popular multi-combinational networks, as listed in Table

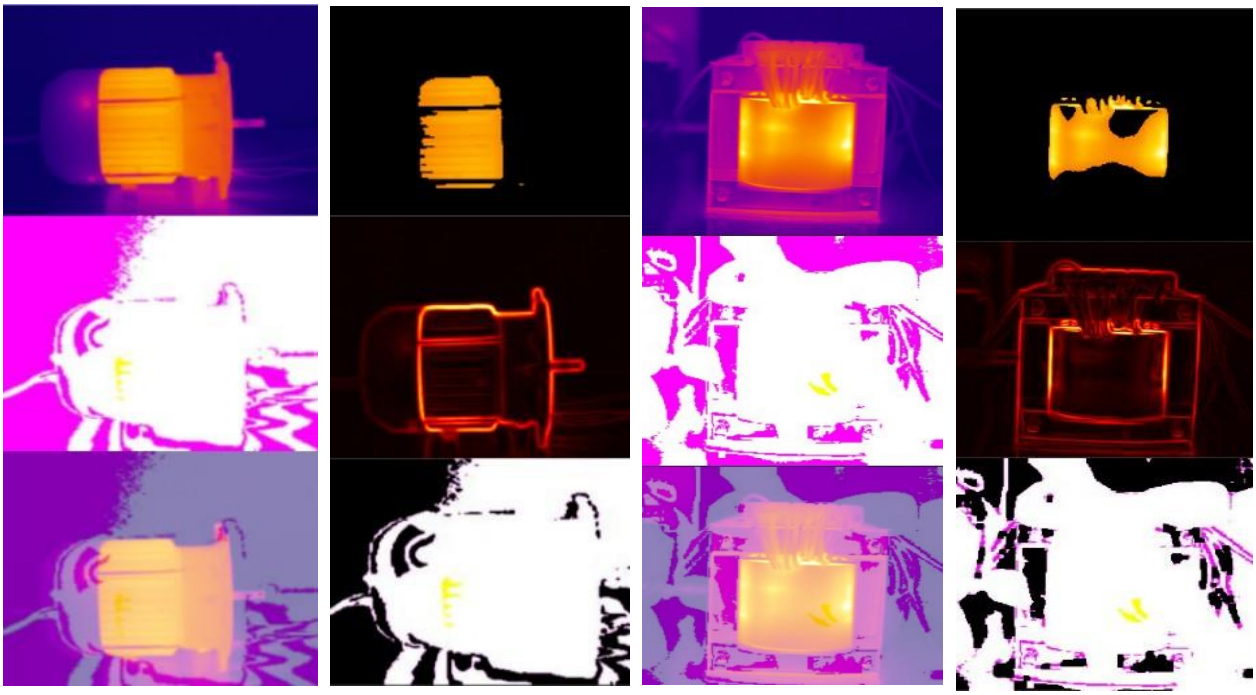

(a) Fault Region Super Imposed Image in Motor (b) Comparing High Intesity Region and FAult region in Motor (c) Fault Region Super Imposed Image in Transformer (d) Comparing High Intesity Region and FAult region in Motor

Fig. 23: Visual Comparison

V. These networks were tested on the current experimental dataset. While these models demonstrated exceptional performance in terms of accuracy, the proposed model showed a slight but consistent improvement in performance metrics, particularly in identifying fault regions. Figure 24 illustrates the stacked accuracy of the tested

Slno	States	Method
1[36]	6	SVM+FCM+NN
2[4]	4	DWT+SVM
3[12]	11	AlexNet+Kmeans+SVM
4[6]	3	NN+Kmeans+BP
5[3]	8	TransferCNN
Proposed Method	11	VGG16+LRP+ Guided Grad CAM

TABLE V: A comparative overview of previous studies

models on the two experimental datasets. The graph clearly shows that the overall accuracy of the proposed method is slightly higher compared to other studies. This indicates that our approach not only competes with but also complements existing methodologies by providing an enhanced fault identification mechanism.

The proposed model's ability to effectively highlight fault regions while maintaining high classification accuracy underscores its potential for practical industrial applications.

V. Conclusion & Future Work

In conclusion, this study introduced an approach for fault diagnosis in rotating machines by harnessing guided thermal images and employing Guided Grad-CAM along with Layer-wise Relevance Propagation (LRP). Leveraging the distinctive features of thermal images captured using thermal camera, this proposed architecture exhibited remarkable accuracy in predicting fault classes and localizing regions of abnormality. The incorporation of Guided Grad-CAM and the unique customization of LRP not only elevated the model's predictive capabilities but also offered valuable visual insights into the root causes of faults, providing a deeper understanding of fault patterns and their spatial distribution within machinery.

Experimental results underscored the effectiveness of the developed architecture in identifying various faults in three-phase induction motors and phase transformers under diverse operational conditions, achieving an impressive accuracy rate and showcasing its potential for real-world fault detection tasks. The precise localization of areas of concern within thermal images holds significant implications for maintenance and decision-making processes, empowering engineers and operators to take prompt corrective actions and minimize downtime.

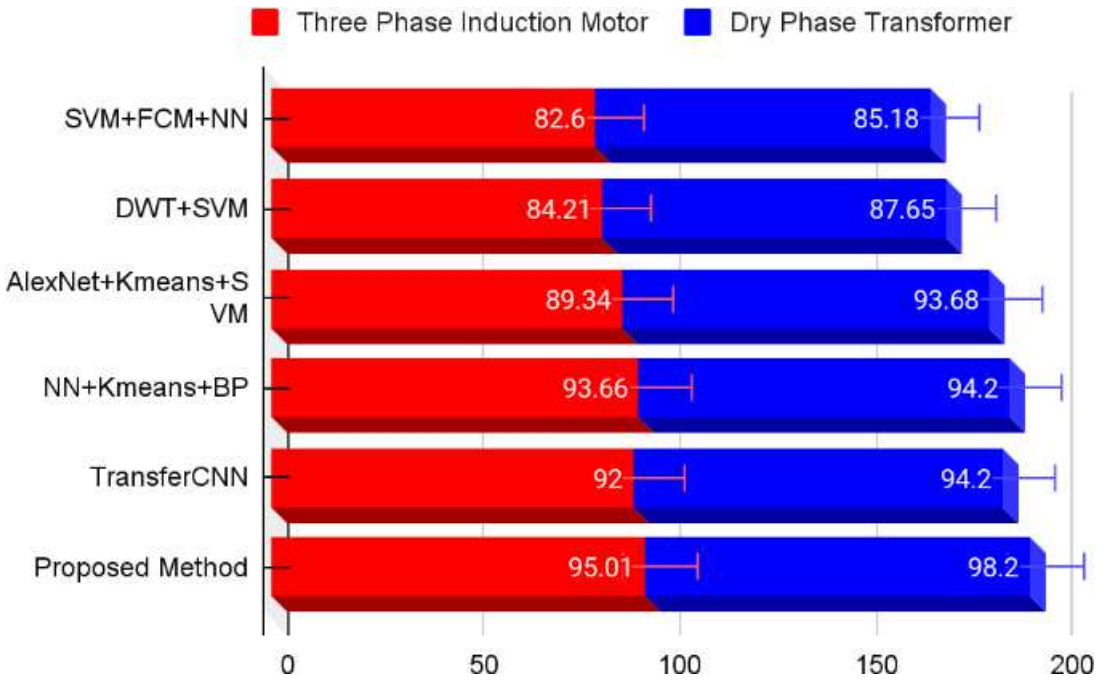

Fig. 24: Accuracy comparison of different models

Looking ahead, several intriguing avenues for future work emerge from the insights gained in this study. One notable direction involves exploring multi-modal approaches by integrating data from different sources, such as vibration sensors or acoustic signals, to enhance the accuracy and robustness of fault diagnosis. Additionally, fine-tuning pre-trained models through transfer learning techniques could potentially bolster the architecture's performance, especially when dealing with limited labelled data.

The prospect of real-time monitoring and anomaly detection beckons, with potential applications in swift machinery health assessment and the identification of fault patterns. Enhancing the model's interpretability and extending its evaluation to a broader range of rotating machinery and fault types represent promising endeavours. These future directions have the potential to refine and broaden the practical utility of fault diagnosis methods for rotating machines, ultimately leading to improved reliability and operational efficiency across industries.

In summary, this study establishes a solid foundation for advancing fault diagnosis practices in machines, with potential applications across industries such as manufacturing, energy, and transportation. The integration of combined LRP and Guided Grad-CAM further enhances the interpretability of fault predictions, opening avenues for continued advancements in the field.

Statements and Declarations

Conflict of Interest

The authors have no conflicts of interest to declare that are relevant to the content of this article.

Funding

No funds, grants, or other support was received.

Data Availability

The data used in this study are available at https://data.mendeley.com/datasets/m4sbt8hbvk/3.

References

[1] Glowacz, A., & Glowacz, Z. (2017). Diagnosis of the three-phase induction motor using thermal imaging. Infrared physics & technology, 81, 7-16.

[2] Al-Musawi, A. K., Anayi, F., & Packianather, M. (2020). Three-phase induction motor fault detection based on thermal image segmentation. Infrared Physics & Technology, 104, 103140.

[3] Shao, H., Xia, M., Han, G., Zhang, Y., & Wan, J. (2020). Intelligent fault diagnosis of rotor-bearing system under varying working conditions with modified transfer convolutional neural network and thermal images. IEEE Transactions on Industrial Informatics, 17(5), 3488-3496.

[4] Choudhary, A., Shimi, S. L., & Akula, A. (2018, September). Bearing fault diagnosis of induction motor using thermal imaging. In 2018 international conference on computing, power and communication technologies (GUCON) (pp. 950-955). IEEE.

[5] Choudhary, A., Mian, T., & Fatima, S. (2021). Convolutional neural network based bearing fault diagnosis of rotating machine using thermal images. Measurement, 176, 109196.

[6] Glowacz, A., & Glowacz, Z. (2017). Diagnosis of the three-phase induction motor using thermal imaging. Infrared physics & technology, 81, 7-16.

[7] Hernández, G. R., Navarro, M. A., Ortega-Sánchez, N., Oliva, D., & Pérez-Cisneros, M. (2020). Failure detection on electronic systems using thermal images and metaheuristic algorithms. IEEE Latin America Transactions, 18(08), 1371-1380.

[8] Lei, Y., Yang, B., Jiang, X., Jia, F., Li, N., & Nandi, A. K. (2020). Applications of machine learning to machine fault diagnosis: A review and roadmap. Mechanical Systems and Signal Processing, 138, 106587.

[9] Janssens, O., Van de Walle, R., Loccufier, M., & Van Hoecke, S. (2017). Deep learning for infrared thermal image based machine health monitoring. IEEE/ASME Transactions on Mechatronics, 23(1), 151-159.

[10] Jia, Z., Liu, Z., Vong, C. M., & Pecht, M. (2019). A rotating machinery fault diagnosis method based on feature learning of thermal images. Ieee Access, 7, 12348-12359.

[11] Najafi, M., Baleghi, Y., Gholamian, S. A., & Mirimani, S. M. (2020, December). Fault diagnosis of electrical equipment through thermal imaging and interpretable machine learning applied on a newly-introduced dataset. In 2020 6th Iranian Conference on Signal Processing and Intelligent Systems (ICSPIS) (pp. 1-7). IEEE.

[12] Khanjani, M., & Ezoji, M. (2021). Electrical fault detection in three-phase induction motor using deep network-based features of thermograms. Measurement, 173, 108622.

[13] Chen, H. Y., & Lee, C. H. (2020). Vibration signals analysis by explainable artificial intelligence (XAI) approach: Application on bearing faults diagnosis. IEEE Access, 8, 134246-134256.

[14] Selvaraju, R. R., Cogswell, M., Das, A., Vedantam, R., Parikh, D., & Batra, D. (2017). Grad-cam: Visual explanations from deep networks via gradient-based localization. In Proceedings of the IEEE international conference on computer vision (pp. 618-626).

[15] Liu, J., Li, Y., & Fu, W. (2019). Fault detection of rotor misalignment in induction motors using infrared thermography. IEEE Access, 7, 22183-22193.

[16] Yin, A., Yan, Y., Zhang, Z., Li, C., & Sánchez, R. V. (2020). Fault diagnosis of wind turbine gearbox based on the optimized LSTM neural network with cosine loss. Sensors, 20(8), 2339.

[17] Qian, W., Li, S., Wang, J., An, Z., & Jiang, X. (2018). An intelligent fault diagnosis framework for raw vibration signals: adaptive overlapping convolutional neural network. Measurement Science and Technology, 29(9), 095009.

[18] Li, L., Zhang, J., He, Z., & Xiang, H. (2021). An Enhanced Remaining Useful Life Prediction Approach for Rotating Machinery Based on EEMD and Data Augmentation. IEEE Access, 9, 59847-59861.

[19] Huang, C., Wang, H., & Zhang, Z. (2019). Multi-sensor data fusion-based fault diagnosis of wind turbine gearboxes using support vector machine and fuzzy clustering. Mechanical Systems and Signal Processing, 117, 100-116.

[20] Liu, Z. H., Chen, L., Wei, H. L., Zhang, Y., Chen, L., & Lv, M. Y. (2022). A Coarse-to-Fine Bilevel Adversarial Domain Adaptation Method for Fault Diagnosis of Rolling Bearings. IEEE Transactions on Instrumentation and Measurement, 71, 1-14.

[21] Johnson, A., Smith, B., & Lee, C. (2020). Transfer Learning for Fault Diagnosis in Rotating Machinery. Proceedings of the International Conference on Machine Learning Applications.

[22] Yongbo, L. I., Xiaoqiang, D. U., Fangyi, W. A. N., Xianzhi, W. A. N. G., & Huangchao, Y. U. (2020). Rotating machinery fault diagnosis based on convolutional neural network and infrared thermal imaging. Chinese Journal of Aeronautics, 33(2), 427-438.

[23] Lopez-Perez, D., & Antonino-Daviu, J. (2017). Application of infrared thermography to failure detection in industrial induction motors: case stories. IEEE Transactions on Industry Applications, 53(3), 1901-1908.

[24] Nasiri, A., Taheri-Garavand, A., Omid, M.,& Carlomagno, G. M. (2019). Intelligent fault diagnosis of cooling radiator based on deep learning analysis of infrared thermal images. Applied Thermal Engineering, 163, 114410.

[25] Glowacz, A. (2021). Fault diagnosis of electric impact drills using thermal imaging. Measurement, 171, 108815.

[26] Choudhary, A., Mian, T., & Fatima, S. (2021). Convolutional neural network based bearing fault diagnosis of rotating machine using thermal images. Measurement, 176, 109196.

[27] Younus, Ali MD, and Bo-Suk Yang. "Intelligent fault diagnosis of rotating machinery using infrared thermal image." Expert Systems with Applications 39.2 (2012): 2082-2091.

[28] Jia, Z., Liu, Z., Vong, C. M., & Pecht, M. (2019). A rotating machinery fault diagnosis method based on feature learning of thermal images. Ieee Access, 7, 12348-12359.

[29] Najafi, Mohamad; Baleghi, Yasser; Mirimani, Seyyed Mehdi (2023), "Thermal image of equipment (Induction Motor) + 40 Ground Truths added", Mendeley Data, V3, doi: 10.17632/m4sbt8hbvk.3

[30] M. Najafi, Y. Baleghi, S. A. Gholamian and S. Mehdi Mirimani, "Fault Diagnosis of Electrical Equipment through Thermal Imaging and Interpretable Machine Learning Applied on a Newly-introduced Dataset," 2020 6th Iranian Conference on Signal Processing and Intelligent Systems (ICSPIS), Mashhad, Iran, 2020, pp. 1-7, doi: 10.1109/ICSPIS51611.2020.9349599.

[31] Ferguson, Max & ak, Ronay & Lee, Yung-Tsun & Law, Kincho. (2017). Automatic localization of casting defects with convolutional neural networks. 1726-1735. 10.1109/BigData.2017.8258115.

[32] Selvaraju, R. R., Cogswell, M., Das, A., Vedantam, R., Parikh, D., & Batra, D. (2017). Grad-cam: Visual explanations from deep networks via gradient-based localization. In Proceedings of the IEEE international conference on computer vision (pp. 618-626).

[33] Lin, M., Chen, Q., & Yan, S. (2013). Network in network. arXiv preprint arXiv:1312.4400.

[34] Huda, A. N., & Taib, S. (2013). Application of infrared thermography for predictive/preventive maintenance of thermal defect in electrical equipment. Applied Thermal Engineering, 61(2), 220-227.

[35] Ahmed, M. M., Huda, A. N., & Isa, N. A. M. (2015). Recursive construction of output-context fuzzy systems for the condition monitoring of electrical hotspots based on infrared thermography. Engineering Applications of artificial intelligence, 39, 120-131.

[36] 2] T. Bai, L. Zhang, L. Duan, J. Wang, NSCT-based infrared image enhancement method for rotating machinery fault diagnosis, IEEE Trans. Instrum. Meas. 65 (10) (2016) 2293–2301.

[37] Janssens, O., Schulz, R., Slavkovikj, V., Stockman, K., Loccufier, M., Van de Walle, R., & Van Hoecke, S. (2015). Thermal image based fault diagnosis for rotating machinery. Infrared Physics & Technology, 73, 78-87.

[38] M. Najafi, Y. Baleghi, Designing an algorithm to automatically detect and classify faults in electrical equipment using thermal images, MSc Thesis, Babol Noshirvani University of Technology, 2017.

[39] Jadin, M. S., Taib, S., & Ghazali, K. H. (2014). Feature extraction and classification for detecting the thermal faults in electrical installations. Measurement, 57, 15-24.

[40] Montavon, G., Binder, A., Lapuschkin, S., Samek, W., & Müller, K. R. (2019). Layer-wise relevance propagation: an overview. Explainable AI: interpreting, explaining and visualising deep learning, 193-209.
[41] Najafi, Mohamad; Baleghi, Yasser; Mirimani, Seyyed Mehdi (2021), "Thermal images dataset, Transformer, 1 phase dry type", Mendeley Data, V3, doi: 10.17632/8mg8mkc7k5.3
[42] Guan, H., Xiao, T., Luo, W., Gu, J., He, R., & Xu, P. (2022). Automatic fault diagnosis algorithm for hot water pipes based on infrared thermal images. Building and Environment, 218, 109111.
[43] Electric Motor Sales Market Size, Share & Trends Analysis Report By Application, By Power Output (Integral HP Output, Fractional HP Output), By Motor Type (Hermetic, AC, DC), By Power Rating, By Voltage (Low, Medium, High), By Region, And Segment Forecasts, 2024 - 2030,https://www.grandviewresearch.com/industry-analysis/electric-motor-market
[44] Metwally, I. A. (2011). Failures, monitoring and new trends of power transformers. IEEE potentials, 30(3), 36-43.
[45] Electronics totorial,https://www.electronics-tutorials.ws/transformer/transformer-loading.html
[46] Rocha, M., Lucas, G., Souza, W., de Castro, B. A., & Andreoli, A. (2021, August). Detection and phase identification of inter-turn short-circuit faults in three-phase induction motors using MEMS accelerometer and Hilbert transform. In 2021 14th IEEE International Conference on Industry Applications (INDUSCON) (pp. 955-961). IEEE.
[47] Transformer,https://www.rgpv.ac.in/campus/BTech_I/transformer.pdf
[48] Mathew, S. (2024). An Overview of Text to Visual Generation Using GAN. Indian Journal of Image Processing and Recognition, 4(3), 1-9.
[49] Rodriguez, P., Sahoo, S., Pinto, C. T.,& Sulowicz, M. (2015, September). Field current signature analysis for fault detection in synchronous motors. In 2015 IEEE 10th International Symposium on Diagnostics for Electrical Machines, Power Electronics and Drives (SDEMPED) (pp. 246-252). IEEE.
[50] Yasid, N. F. M., Yousof, M. F. M., Rahman, R. A., Zainuddin, H., & Ghani, S. A. (2019). The effect of short circuit fault on one winding to other windings in FRA. International Journal of Power Electronics and Drive Systems (IJPEDS), 10(2), 585.
[51] Hegde, V., & Sathyanarayana Rao, M. G. (2017). Detection of stator winding inter-turn short circuit fault in induction motor using vibration signals by MEMS accelerometer. Electric Power Components and Systems, 45(13), 1463-1473.
[52] Elctronics Tutorials https://www.electronics-tutorials.ws/transformer/transformer-loading.html
[53] Jin, C., Ompusunggu, A. P., Liu, Z., Ardakani, H. D., Petré, F., & Lee, J. (2015). Envelope analysis on vibration signals for stator winding fault early detection in 3-phase induction motors. International Journal of Prognostics and Health Management, 6(1).
[54] Abitha Memala, W., & Rajini, V. (2017). Wavelet-Based Induction Motor Fault Diagnosis Using Zero Sequence Current. Journal of Computational and Theoretical Nanoscience, 14(1), 411-420.

ABOUT THE AUTHORS

Sibi Mathew completed M.Tech in Computer Science and Engineering at TKM College of Engineering, Kollam, Kerala, India. His research interests include Image Processing, Image-based Fault Diagnosis, Deep Learning, and Machine Learning. He holds a Bachelor's degree in Computer Science and Engineering from Amal Jyothi College of Engineering. He is passionate about leveraging advanced technologies to solve real-world problems in diverse domains.

Aneesh G. Nath completed his Ph.D. degree in computer science and engineering at IIT (BHU) Varanasi, Varanasi, India. He also has an M.Tech. degree in computer engineering from the National Institute of Technology Karnataka (NITK), in 2014. He is currently an Associate Professor with the Department of Computer Science and Engineering, TKM College of Engineering, Kollam, Kerala. His current research interests include machine learning, data science, signal processing, and optimization.

Shyna A completed her M.Tech from Cochin University of Science and Technology and B.Tech from the University of Kerala. She is currently working as an Assistant Professor in the Department of Computer Science and Engineering at TKM College of Engineering, Kollam, India. Her area of research interests includes Image Processing, Soft Computing, and Machine Learning.